Article published online: 2021-07-19

Imaging in congenital inner ear malformations—An algorithmic approach

Abhinav C Bhagat, Jyoti Kumar, Anju Garg, Anjali Prakash, Ravi Meher[1], Shivali Arya

Departments of Radiodiagnosis and [1]ENT, Maulana Azad Medical College and Lok Nayak Hospital, New Delhi, India

Correspondence: Dr. Jyoti Kumar, Department of Radiodiagnosis, Maulana Azad Medical College and Associated Lok Nayak Hospital, New Delhi - 110 002, India. E-mail: drjyotikumar@gmail.com

Abstract

Malformations of the inner ear are an important cause of congenital deaf-mutism. Arrest in embryologic development of inner ear during various stages gives rise to the variety of malformations encountered. Current treatment options include hearing aids, cochlear implants, and auditory brainstem implants (ABI). With the advent of cochlear implant surgery and ABI, decent functional outcomes can be obtained provided such cases are diagnosed correctly and timely. To that end, high-resolution computed tomography (HRCT) has a fundamental role in the assessment of these conditions, ably supplemented by magnetic resonance imaging (MRI). The purpose of this pictorial essay is to illustrate the imaging features of inner ear anomalies in children with congenital deaf-mutism as per the latest terminology and classification and provide an algorithmic approach for their diagnosis.

Key words: Cochlear implant; congenital deaf-mutism; high-resolution computed tomography; inner ear; Mondini, magnetic resonance imaging

Introduction

The embryologic development of inner ear occurs in a predefined sequence starting in the 3rd week of intrauterine life. Depending upon the timing of insult in utero, anatomically different anomalies may manifest. However, only a minority (20–30%) will show radiologic abnormality on imaging.[1] This has been attributed to changes occurring at the cellular or microscopic levels which are beyond the resolving power of current imaging techniques. These children usually present with congenital deaf-mutism in the first few years of life. Often these children can have systemic abnormalities in association with inner ear malformations; hence a complete physical examination must be performed.

Currently, three treatments are available for hearing rehabilitation in such patients: Hearing aids, cochlear implants, and auditory brainstem implants (ABI). Cochlear implantation has been proven to be clinically effective and cost-effective in children with severe to profound bilateral sensorineural hearing loss.[2] Due to the widespread adoption of cochlear implantation, high-resolution computed tomography (HRCT) temporal bone and magnetic resonance imaging (MRI) have become invaluable in the imaging evaluation and characterization of inner ear anomalies. HRCT provides an excellent depiction of the bony labyrinth, osseous details as well as variant anatomy, whereas MRI demonstrates membranous labyrinth, vestibulocochlear nerve and brain pathology to good effect.[3] These findings can aid in the decision between cochlear implant and ABI. The choice between these two modalities for preoperative imaging varies among

Access this article online

Quick Response Code:

Website: www.ijri.org

DOI: 10.4103/ijri.IJRI_58_19

Cite this article as: Bhagat AC, Kumar J, Garg A, Prakash A, Meher R, Arya S. Imaging in congenital inner ear malformations—An algorithmic approach. Indian J Radiol Imaging 2020;30:139-48.

Received: 06-Jun-2019 **Revised:** 08-Oct-2019
Accepted: 30-Nov-2019 **Published:** 13-Jul-2020

institutions, with some relying primarily on either CT or MR imaging whilst others preferring to use both these imaging modalities in a complementary fashion.[4,5] If a cochlear implant is planned, imaging findings impact the surgical approach and also the type of electrode used.[6]

This review article describes the spectrum of inner ear anomalies one is likely to encounter on imaging of children with congenital deaf-mutism. The terminology used draws upon from the latest classification system of Sennaroglu.[7] Additionally, it provides an algorithmic approach for the classification of the same.

Normal Anatomy of Inner Ear

The inner ear is divided into the bony and membranous labyrinth. The bony labyrinth is well-demonstrated by HRCT and consists of vestibule, cochlea, semicircular canals, vestibular aqueduct, and cochlear aqueduct [Figures 1 and 2].

The membranous labyrinth is housed within the bony labyrinth with intervening space bathed in the perilymph. It consists of utricle and saccule, cochlear duct, semicircular ducts, and endolymphatic duct and sac. The fluid contained within is called endolymph. MRI is useful for demonstrating the membranous labyrinth.

Internal auditory canal (IAC)

The IAC is a bony canal 2–8 mm wide that courses through the petrous bone between the cerebellopontine angle and labyrinth and transmits the facial and vestibulocochlear nerves. The cochlea lies anterior and vestibule posterior to it. The vestibulocochlear nerve divides into three branches within the IAC: Cochlear nerve, superior vestibular nerve, and inferior vestibular nerve. The IAC is divided into four compartments by a horizontal falciform crest and an incomplete vertical Bill's bar, the latter is occasionally visualized [Figure 3]. The facial nerve and cochlear nerve occupy the anterosuperior and anteroinferior compartments, respectively. The superior and inferior vestibular nerves are housed in posterosuperior and posteroinferior compartments, respectively.

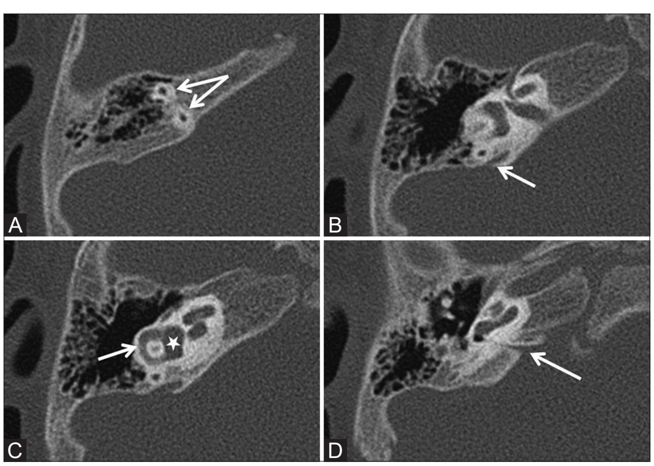

Figure 1 (A-D): Axial CT images through temporal bone showing normal inner ear structures. Superior semicircular canal (A), vestibular aqueduct (B), lateral semicircular canal (arrow in C), vestibule (star) and cochlear aqueduct (D)

Cochlea

Anterior to the IAC is cochlea, which is a spiral canal that winds 2½ to 2¾ times around the central bony modiolus. On HRCT, the mid-modiolar view demonstrates the modiolus as a central osseous density, interscalar septa which divide the cochlea into the basal, middle, and apical turns and cochlear aperture transmitting cochlear nerve from IAC to the cochlea. Section through the round window niche, which lies just inferior to the mid-modiolar section, demonstrates the basal, middle and apical turns separately [Figure 2]. Besides, Stenvers projection which is obtained by taking sections parallel to the long axis of petrous bone can also show normal cochlear turns to good effect. The cochlear lumen is divided by osseous spiral lamina into superior scala vestibuli and inferior scala tympani.

Cochlear aqueduct is a bony canal that is filled with loose connective tissue and connects the scala tympani with

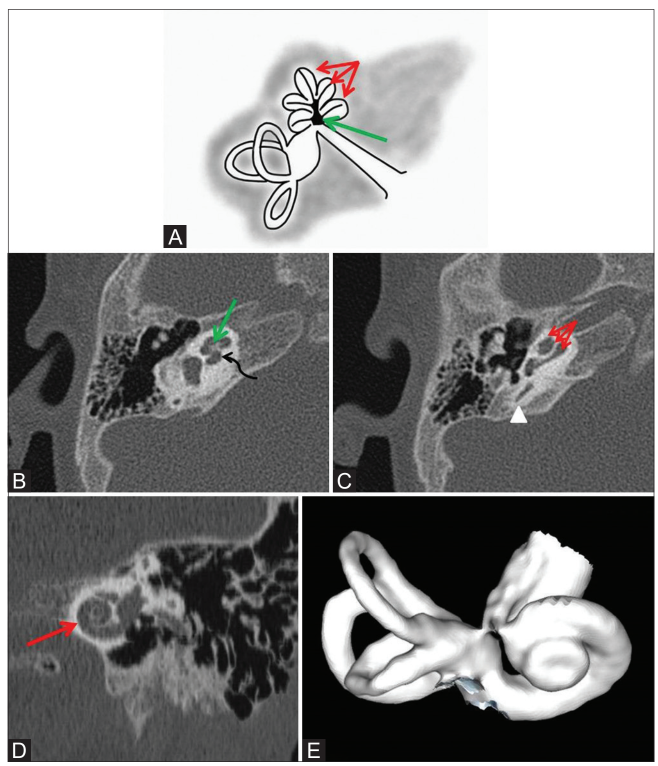

Figure 2 (A-E): Schematic illustration of the normal inner ear (A) and normal cochlear anatomy at level of modiolus (B), and round window niche (C). Minimum intensity projection (MinIP) image of Stenvers projection nicely shows cochlear turns (D). 3D volume rendering of the normal inner ear (E). Green arrow: Modiolus, curved black arrow: Cochlear aperture, red arrows: Cochlear turns, arrowhead: Posterior semicircular canal

subarachnoid space adjacent to pars nervosa of jugular foramen [Figures 1d and 4]. It runs parallel and inferior to the IAC with a wider medial opening which tapers off laterally as it courses into the petrous bone.

Vestibule and semicircular canals

The vestibule lies posterior to the IAC and joins with the cochlea, semicircular canals, and vestibular aqueduct. It houses the utricle and saccule. The vestibular aqueduct is a bony canal containing endolymphatic duct which connects the utricle and saccule with endolymphatic sac in the epidural space of posterior cranial fossa [Figures 1b and 4]. It courses postero-lateral and parallel to the posterior semicircular canal. Its normal diameter is 1.5 mm or less and is nearly the same as that of the posterior semicircular canal. The three semicircular canals (superior, lateral, and posterior) house the semicircular ducts which join the vestibule. The posterior part of the superior semicircular canal joins with the upper part of the posterior semicircular canal to form the crus commune.

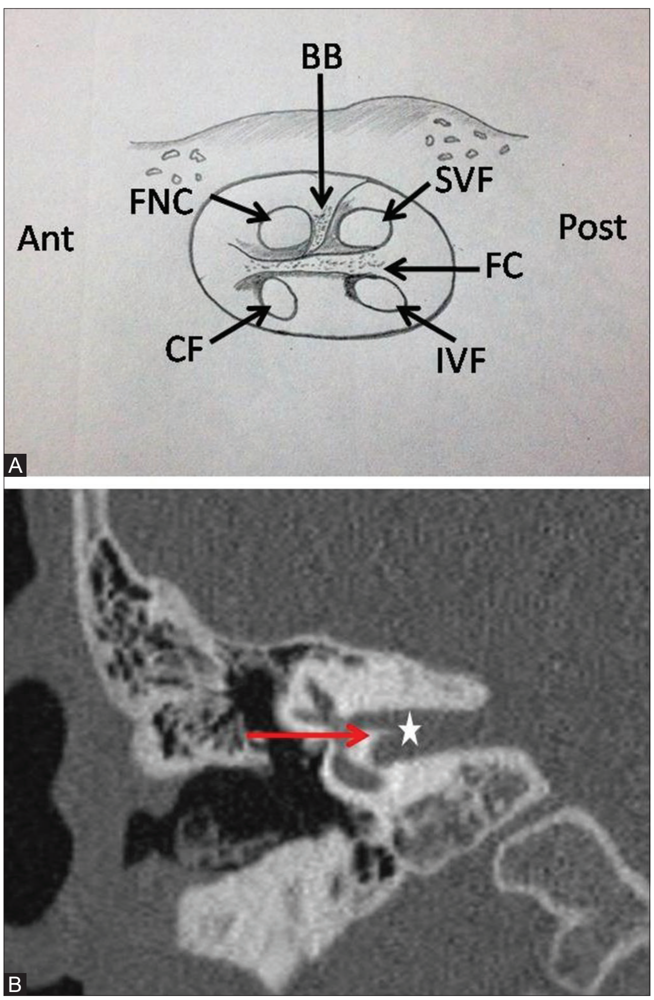

Figure 3 (A and B): Schematic diagram (A) shows the cross-section of internal auditory canal with its contents. Coronal CT image (B) of temporal bone shows horizontal falciform crest (arrow) at the lateral end of the internal auditory canal (star) BB: Bill's bar, FC: Falciform crest, FNC: Facial nerve canal, CF: Cochlear fossa, SVF: Superior vestibular fossa, IVF: Inferior vestibular fossa

Imaging Technique

CT technique

HRCT of the temporal bone using an MDCT scanner (64 slices or more) provides good anatomic details for the evaluation of inner ear.

- Scan plane: Axial scans through the temporal bone are acquired (512 × 512 matrix) from the top of the petrous apex to the inferior tip of the mastoid bone
- Slice thickness: The raw axial image dataset is reconstructed with a section thickness of 0.6 mm. Coronal images are reconstructed from the anterior margin of the petrous apex to the posterior margin of the mastoid. Sagittal images can be reformatted whenever required
- Windowing and centering: Images are displayed at window centering level of 700 HU and a window width of 4000 HU. 3D surface reconstruction and volume-rendered images can also be obtained.

MR technique

3T MR imaging system provides excellent images for inner-ear examinations.

- Heavily T2-weighted sequences in the axial plane: Thin section axial images (0.4–0.7 mm) of heavily T2-weighted 3D sequences such as SPACE, CISS (Siemens); FIESTA (GE); VISTA (Philips) are used for imaging the inner ear [Figures 5; 6A and B]. The high-resolution 3D dataset can be used for generating multi-planar reformatted images
- Heavily T2-weighted sequences in the sagittal oblique plane for vestibulocochlear nerves: Oblique sagittal

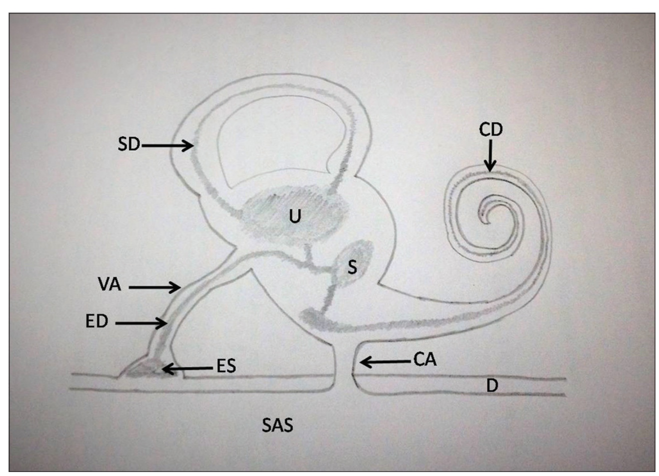

Figure 4: Schematic illustration of inner ear structures showing the location of vestibular and cochlear aqueduct. VA: Vestibular aqueduct, ED: Endolymphatic duct, ES: Endolymphatic sac, CA: Cochlear aqueduct, D: Dura mater, SAS: Subarachnoid space, CD: Cochlear duct, SD: Semicircular duct, U: Utricle, S: Saccule

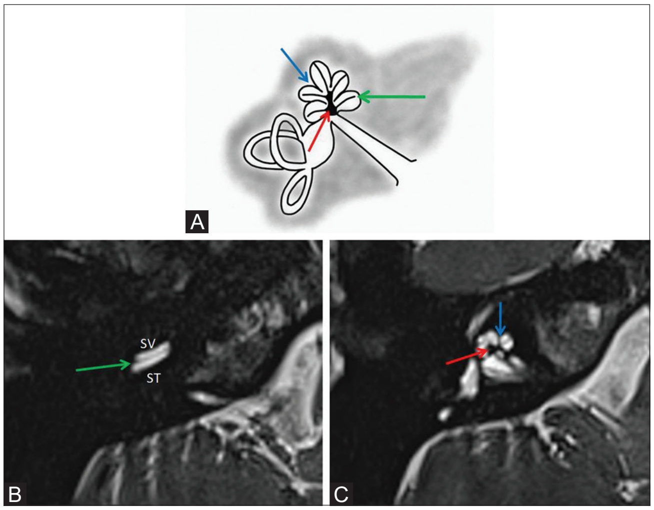

Figure 5 (A-C): Schematic illustration of normal inner ear (A) and axial 3D T2W SPACE images (B and C) through posterior fossa show osseous spiral lamina of basal cochlear turn (green arrow) separating the scala vestibuli (SV) and scala tympani (ST), interscalar septum between middle and apical turn of cochlea (blue arrow) and central modiolus (red arrow)

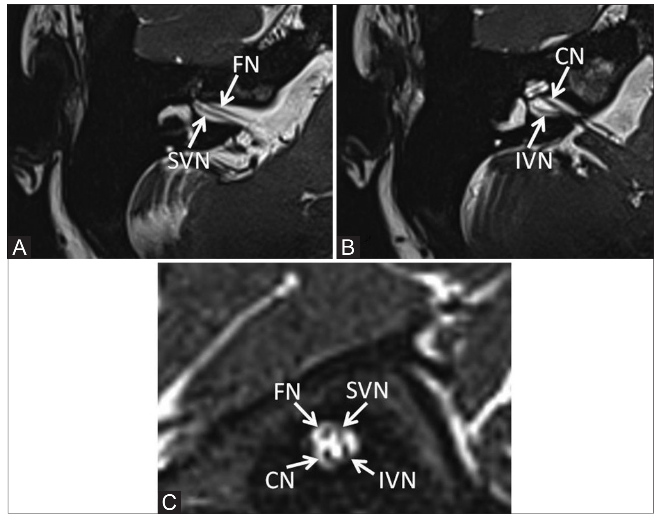

Figure 6 (A-C): Axial 3D T2W SPACE images through superior (A) and inferior (B) part of IAC and oblique sagittal image (C) through IAC show the facial nerve and three divisions of vestibulocochlear nerve. FN: Facial nerve, SVN: Superior vestibular nerve, CN: Cochlear nerve, IVN: Inferior vestibular nerve

images are obtained in the plane perpendicular to the course of the nerves in internal auditory canal and exquisitely demonstrate the facial and vestibulocochlear nerves within the IAC [Figure 6C]

- Imaging for the brain: The examination must be supplemented by routine imaging of the brain in all patients to exclude lesions of the central nervous system responsible for hearing loss; contrast may be administered when deemed necessary.

Imaging Spectrum

According to current classification, inner ear malformations are divided into eight types. Each group of malformation presents with similar clinical findings and has similar treatment options and prognostic implications. These include

1. Complete labyrinthine aplasia (Michel aplasia)
2. Rudimentary otocyst
3. Cochlear aplasia
4. Common cavity
5. Cochlear hypoplasia
6. Incomplete partition of cochlea
7. Enlarged vestibular aqueduct
8. Cochlear aperture abnormalities.

Complete labyrinthine aplasia

Also known as Michel aplasia, it is the most severe end of the spectrum resulting from developmental arrest during the 3rd week of gestation.[8]

Imaging findings

- Complete absence of inner ear structures [Figure 7]
- Can be unilateral or bilateral. When unilateral, the contralateral inner ear is often malformed[9]
- The petrous bone and otic capsule may be hypoplastic or aplastic.[10]

Treatment

Since there is no inner ear, a cochlear implant is contraindicated and ABI is the only available treatment.

Rudimentary otocyst

A rudimentary otocyst represents an incomplete millimetric otic capsule (round or ovoid in shape) with the absence of internal auditory canal.[7]

Like complete labyrinthine aplasia, ABI is the only treatment option.

Cochlear aplasia

Imaging findings

- There is complete agenesis of the cochlea, with or without the affliction of other inner ear structures [Figure 8]. Two subgroups are described: Cochlear aplasia with a normal labyrinth and cochlear aplasia with a dilated vestibule (CADV)
- The labyrinthine segment of facial nerve shows anterior displacement occupying the site where normal cochlea should have been.

Imaging differential

Labyrinthitis ossificans: Absence of bulge of the cochlear promontory in the medial wall of middle ear differentiates cochlear aplasia from labyrinthitis ossificans.[9]

Treatment

The absence of cochlea precludes a cochlear implant, ABI being the sole treatment option.

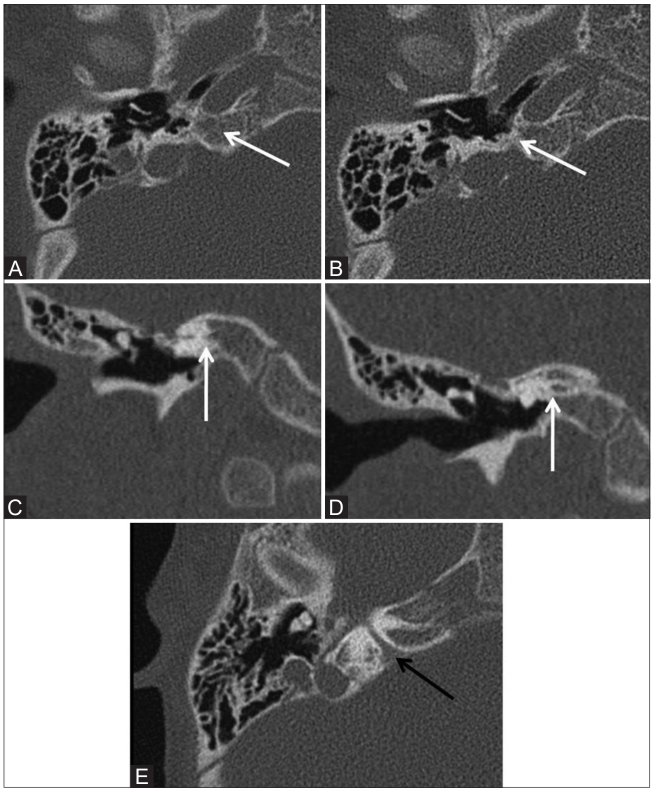

Figure 7 (A-E): Complete labyrinthine aplasia. Axial (A, B and E) and coronal (C and D) CT images reveal complete absence of inner ear structures and hypoplastic petrous bone (white arrows) with absent bulge of promontory on the right side and stenotic IAC (black arrow)

Common cavity

Imaging findings

- Cochlea and vestibule are not identified as separate structures but are fused together to form a single cavity [Figure 9]
- Associated malformations of semicircular canals are common.

Imaging differential

Cochlear aplasia with dilated vestibule (CADV): In the common cavity, the internal auditory canal enters at its center whereas the vestibule is positioned postero-lateral to the fundus of the internal auditory canal in CADV. While a cochlear implant can be attempted in the common cavity, it is contraindicated in CADV. However, it may be difficult to differentiate between these two entities.[7]

Treatment

Cochlear implant is the primary treatment option; ABI is attempted in case of neural deficiency or poor response to cochlear implant.

Cochlear hypoplasia

Imaging findings

- Cochlea and vestibule can be differentiated but cochlear external dimensions are less than normal with internal architecture often not made out[7]
- It may appear bud-like or cystic hypoplastic with absent or shortened modiolus and interscalar septa. The number of cochlear turns may be reduced [Figure 10]
- Four subtypes are described based on cochlear morphology[7]
    - CH-I: cochlea appears small bud-like
    - CH-II: cochlea appears cystic with small dimensions; however, external outline is normal
    - CH-III: cochlea has reduced number of turns (<2) with small dimensions; however, external outline is normal
    - CH-IV: cochlea has a normal basal turn; however, middle and apical turns are hypoplastic.

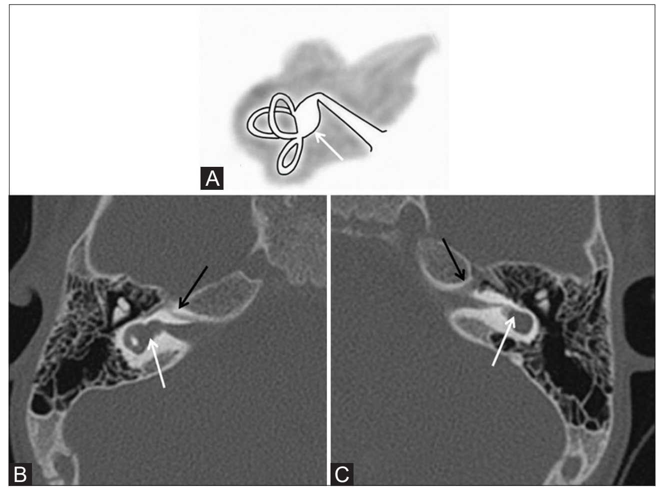

Figure 8 (A-C): Cochlear aplasia. Schematic illustration (A), right (B) and left (C) axial CT images show cochlear aplasia with dilated vestibule (white arrows). Note the anterior displacement of the labyrinthine segment of bilateral facial nerve (black arrows)

Imaging differential

Incomplete partition deformity: The cochlear dimensions are normal in the incomplete partition deformity as opposed to reduced dimensions in cochlear hypoplasia.

Treatment

It varies from stapedotomy, hearing aids and cochlear implants. If the cochlear nerve is deficient ABI is the only available option.

Incomplete partition (IP)

In this group, cochlea and vestibule are seen as distinct structures but show variable internal architecture deformities. Cochlear size is normal, unlike cochlear hypoplasia. It is subdivided into three groups: IP-I, IP-II, and IP-III.

Imaging findings

A. Incomplete partition-I [Figure 11]
    - Previously called cystic cochleovestibular malformation, cochlea appears cystic with the absence of modiolus and internal architecture but seen separate from the vestibule

- None of the cochlear turns is identified; however, external dimensions of the cochlea are normal
- The vestibule is often enlarged and dysplastic, however, the vestibular aqueduct is usually not dilated. The internal auditory canal is usually enlarged
- The cochlear nerve may or may not be present
- These patients are at an increased risk of meningitis and CSF gusher during cochlear implant surgery[7,11]
- It may be associated with syndromes such as Klippel Feil syndrome [Figure 12].

B. Incomplete partition-II [Figure 13]

- The cochlear apex assumes a cystic appearance due to a defect in the apical part of modiolus and interscalar septa leading to confluent middle and apical turns. Basal turn is normally developed
- The term Mondini deformity is used when this deformity is present with a mildly dilated vestibule and an enlarged vestibular aqueduct

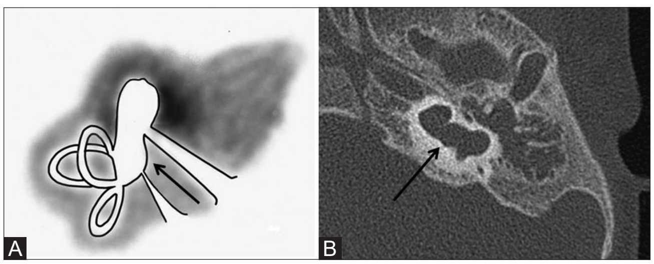

Figure 9 (A and B): Common cavity. Schematic diagram (A) and axial CT (B) reveal a cystic structure (arrow) without internal architecture representing the assimilation of cochlea and vestibule

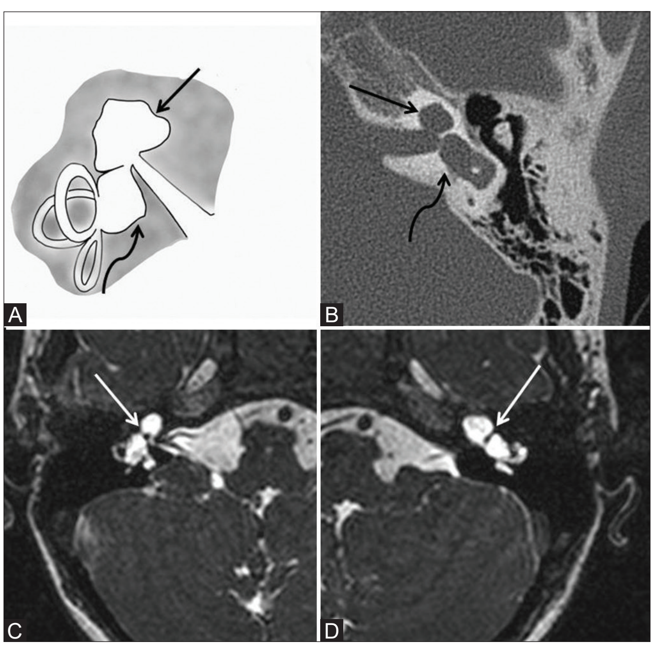

Figure 11 (A-D): Incomplete partition-I. Schematic illustration (A) and axial CT image (B) reveal empty cystic cochlea with no internal architecture (straight arrow) and dilated dysplastic vestibule (curved arrow). Axial T2W 3D CISS MR images (C and D) in a different patient show bilateral deformity (arrows)

- The cochlear nerve is always present.

C. Incomplete partition-III [Figure 14]

- Associated with X-linked deafness, it is the rarest

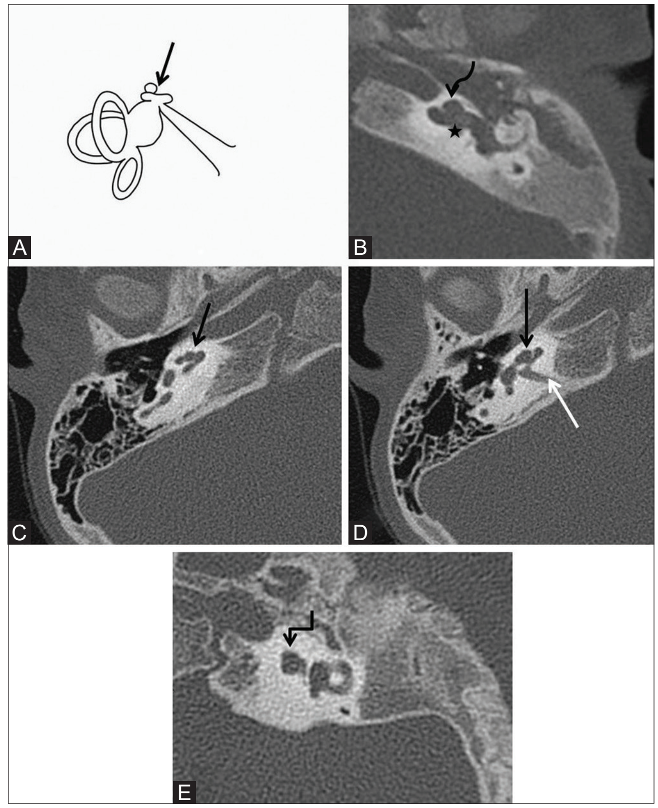

Figure 10 (A-E): Cochlear hypoplasia. Schematic diagram (A) shows cochlea with reduced dimensions (arrow). Axial CT image (B) reveals normal basal turn (star) with hypoplastic middle and apical turns (curved arrow) in cochlear hypoplasia type IV. Axial CT images (C and D) show an overall small cochlea with less than two turns (black arrows) suggesting cochlear hypoplasia type III. Stenosis of IAC is also seen (white arrow). Cochlear hypoplasia type II (E) reveals an overall small cochlea with cystic appearance (square arrow)

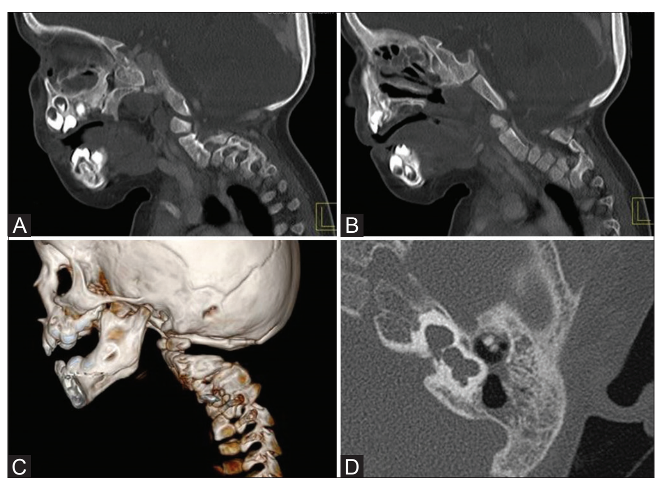

Figure 12 (A-D): Incomplete partition-I in association with Klippel-Feil syndrome. Sagittal CT reformats (A and B) and VRT image (C) of the cervical spine show fusion segmentation anomalies of cervical vertebrae with an associated incomplete partition-I malformation (D)

of the partition anomalies of cochlea in which the interscalar septa are present; however, modiolus is completely absent

- The external dimensions of the cochlea are more or less normal. There is a bulbous enlargement of internal auditory canal with defective lamina cribrosa
- The cochlear nerve is always present.

Imaging differential

Cochlear hypoplasia: It can be differentiated from incomplete partition abnormality on the basis of reduced cochlear dimensions in cochlear hypoplasia.[7]

Treatment

It varies between hearing aids and cochlear implants. ABI is performed in cases of poor response to a cochlear implant or nerve deficiency (IP-I).

Enlarged vestibular aqueduct

Imaging findings

- The vestibular aqueduct is said to be enlarged if its width exceeds 1.5 mm at the midpoint between posterior labyrinth and operculum [Figure 15] or when it exceeds that of the adjacent posterior semicircular canal[12]
- It can be bilateral in upto 90% of patients[13]
- The cochlea, vestibule, and semicircular canals are normal

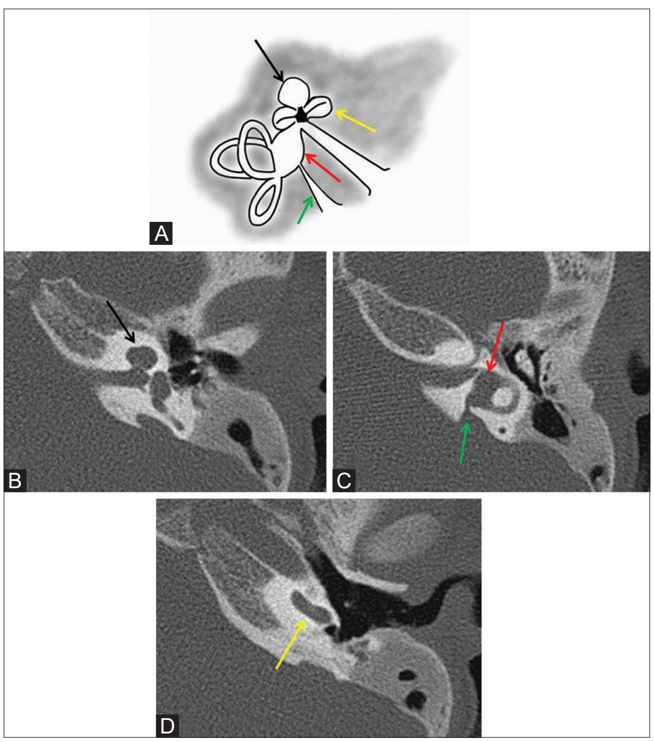

Figure 13 (A-D): Incomplete partition-II. Schematic illustration (A) and axial CT images (B-D) show fusion of middle and apical turns of cochlea resulting in cystic apex (black arrow), mildly dilated vestibule (red arrow) with enlarged vestibular aqueduct (green arrow), and normal-appearing basal turn of cochlea (yellow arrow) forming Mondini's triad

- Pöschl projection can be used to demonstrate the entire course of the vestibular aqueduct on a single section which is not possible on axial sections due to its oblique orientation [Figure 16]. It is a 45° oblique reformat perpendicular to the long axis of the petrous bone. More commonly used for the evaluation of superior semicircular canal dehiscence, it is also useful for the assessment of vestibular aqueduct particularly in cases of borderline enlargement.[12,14]

Treatment

The severity of hearing loss dictates management, hearing aids being used for mild to moderate hearing loss and cochlear implants for severe cases.

Abnormalities of cochlear aperture

Imaging findings

- Cochlear aperture transmits the cochlear nerve from the internal auditory canal to cochlea. Hypoplasia of the cochlear aperture is defined by width less than 1.4 mm and aplasia is characterized by replacement of cochlear aperture with bone[7]
- Concomitant narrowing of the internal auditory canal may also be present [Figure 17]
- The cochlear nerve may be hypoplastic or absent. Cohlear nerve hypoplasia is diagnosed if its size is less than ipsilateral normal facial nerve or contralateral normal cochlear nerve. Cochlear nerve hypoplasia or aplasia may occur without abnormality of cochlea or cochlear aperture.

Treatment

Hypoplastic cochlear aperture with cochlear nerve hypoplasia is initially treated by hearing aid followed by cochlear implant in case of a suboptimal response. ABI is the only possible treatment in cases of cochlear nerve aplasia.

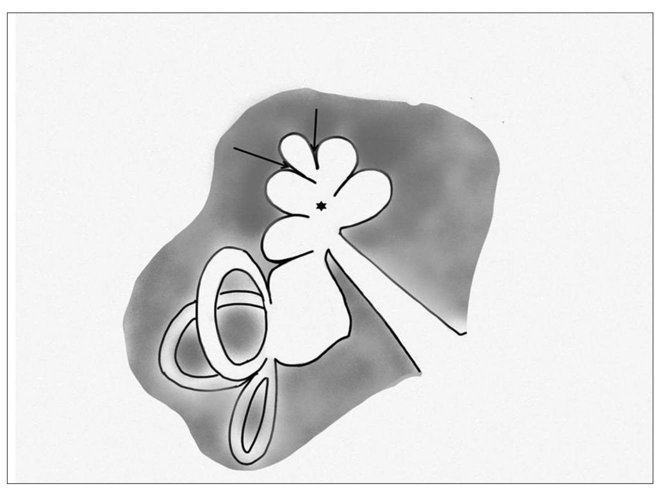

Figure 14: Incomplete partition-III. Schematic illustration shows cochlea with absent modiolus (*) but interscalar septa (arrows) are present

Abnormalities of semicircular canals

Malformations of semicircular canals may be seen in isolation or in combination with cochlear and vestibular anomalies.

- They can be absent, hypoplastic, or dilated
- Any of the three canals may be affected, and it is not uncommon for them to be affected in combination. The most frequently involved is the lateral semicircular canal (as it is the last to develop embryologically) wherein the lateral canal is assimilated within a dilated dysplastic vestibule, the so-called vestibule-lateral semicircular canal dysplasia [Figure 18].

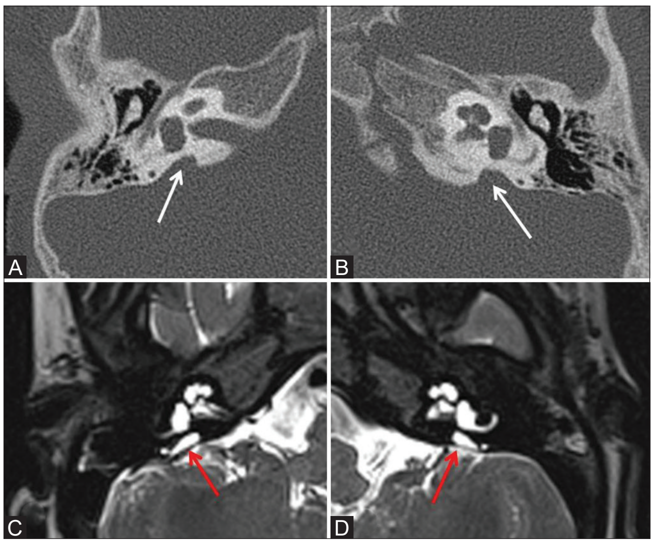

Figure 15 (A-D): Enlarged vestibular aqueduct. Axial CT images (A and B) show dilated vestibular aqueduct bilaterally (white arrows). Axial T2W 3D CISS MR images (C and D) in a different patient show the same finding (red arrows)

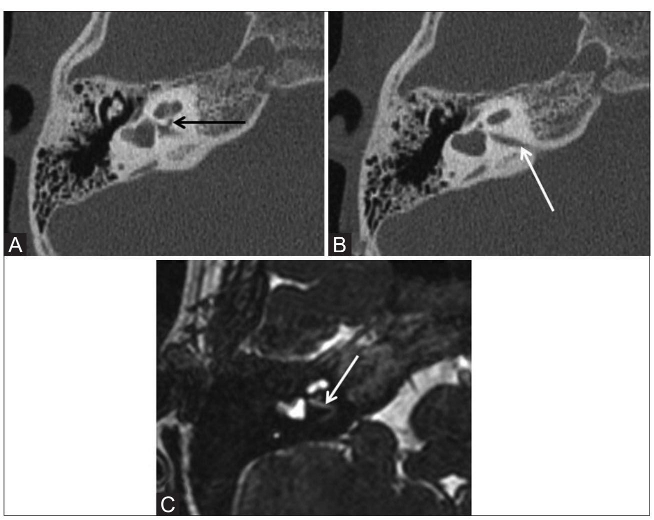

Figure 17 (A-C): Hypoplasia of cochlear aperture. Axial CT images (A and B) show hypoplasia of the cochlear nerve canal (black arrow) with associated stenosis of IAC (white arrow). Axial T2W 3D CISS MR image (C) in the same patient shows absence of neural elements within the stenotic IAC (arrow)

Abnormalities of IAC

IAC abnormalities may occur as part of other inner ear malformations or in isolation. Normal diameter is stated to be between 2 and 8 mm.

- *Stenosis* is defined as an IAC diameter of less than

Figure 16: Oblique course of normal vestibular aqueduct (arrow) in Pöschl projection

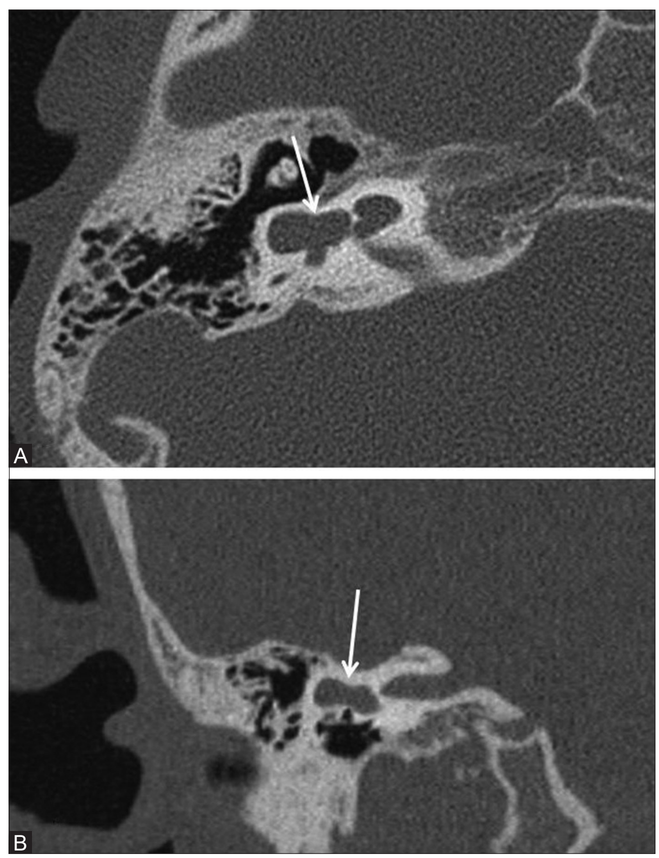

Figure 18 (A and B): Vestibule-lateral semicircular canal dysplasia. Axial (A) and coronal (B) CT images show the fusion of lateral semicircular canal with dysplastic vestibule (arrows) in a case of incomplete partition-I

2 mm. It is frequently associated with cochlear nerve deficiency or absence
- *Dilated IAC* has been found to be associated with IP-I malformation but may also be seen in isolation
- *Duplication of IAC* [Figure 19] is a relatively uncommon condition in which two bony canals are seen within the petrous bone on HRCT of which one continues as the facial nerve canal and the other terminates in cochlea and vestibule.[15,16]

An algorithmic approach to classification and diagnosis of inner ear anomalies is presented in Figure 20.

Conclusion

HRCT and MR imaging have evolved as indispensable imaging modalities for the assessment of congenitally deaf-mute children. Inner ear malformations, when present, can be classified using this algorithmic approach as described above. It is imperative to use standard and correct terminology while describing these malformations because it can have a significant impact on the management and prognosis of these children. Sound knowledge of inner ear anatomy, appropriate use of classification terminology and

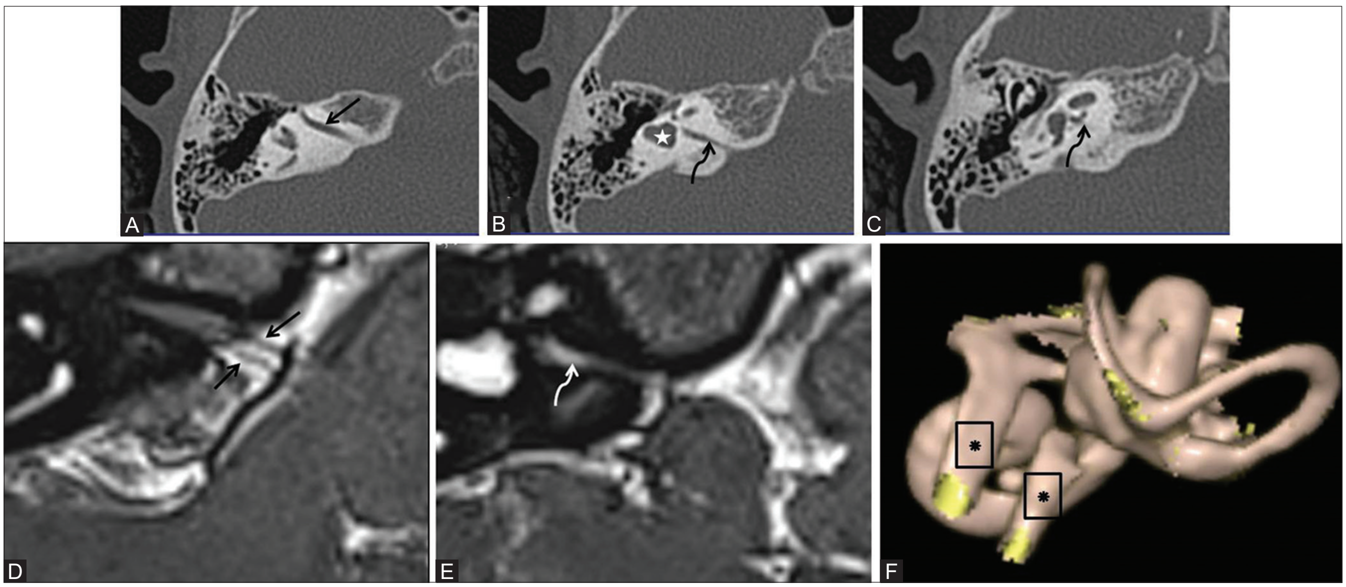

Figure 19 (A-F): Duplicated IAC. Axial CT images (A-C) show two narrow bony canals with anterosuperior canal continuing as facial nerve (straight arrow) and posteroinferior canal extending to labyrinth (curved arrow). Vestibule-lateral semicircular canal dysplasia is also seen (star). Axial 3D T2W SPACE images (D and E) in the same patient show two nerves (straight arrows) entering the superior canal with the narrow empty inferior canal (curved arrow). 3D volume-rendered image (F) in a different patient shows double IAC (asterisks)

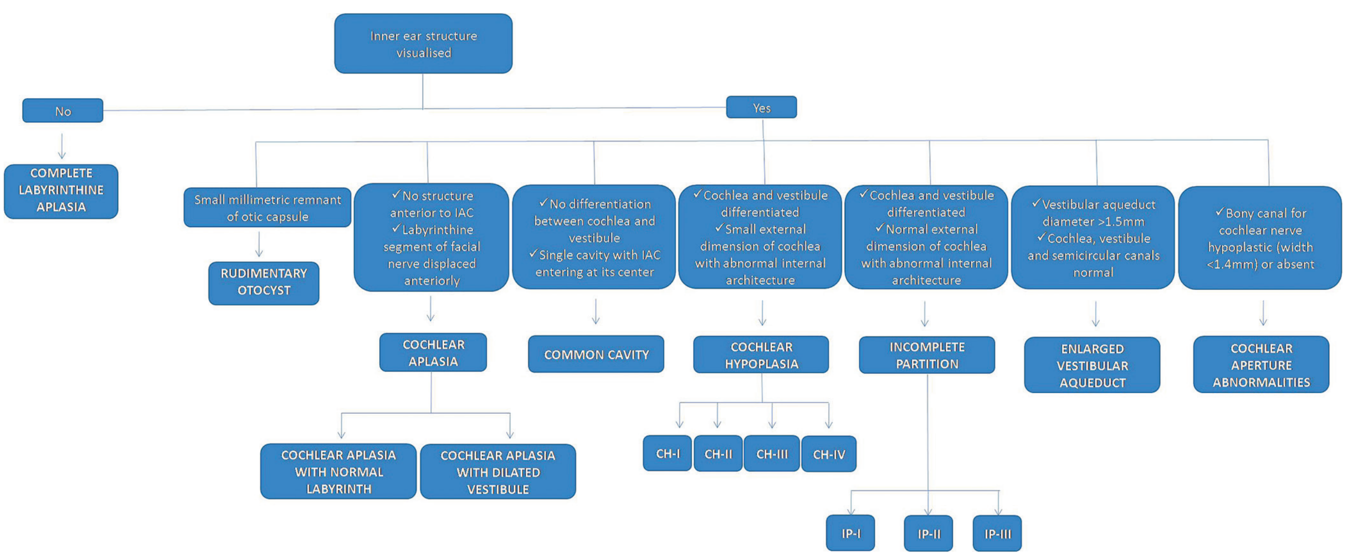

Figure 20: Algorithmic approach to classification and diagnosis of major inner ear malformations

clear communication with ENT surgeons reduces ambiguity and chances of unnecessary or inappropriate interventions.

Financial support and sponsorship

Nil.

Conflicts of interest

There are no conflicts of interest.

References

1. Huang BY, Zdanski C, Castillo M. Pediatric sensorineural hearing loss, Part 1: Practical aspects for neuroradiologists. Am J Neuroradiol 2012;33:211-17.
2. Chen MM, Oghalai JS. Diagnosis and management of congenital sensorineural hearing loss. Curr Treat Options Pediatr 2016;2:256-65.
3. Bartel-Friedrich S, Wulke C. Classification and diagnosis of ear malformations. GMS Curr Top Otorhinolaryngol Head Neck Surg 2007;6:Doc05.
4. Young JY, Ryan ME, Young NM. Preoperative imaging of sensorineural hearing loss in pediatric candidates for cochlear implantation. Radiographics 2014;34:E133-49. doi: 10.1148/rg.345130083.
5. Digge P, Solanki RN, Shah DC, Vishwakarma R, Kumar S. Imaging Modality of Choice for Pre-Operative Cochlear Imaging: HRCT vs. MRI Temporal Bone. J Clin Diagn Res 2016;10:TC01-TC04. doi: 10.7860/JCDR/2016/18033.8592.
6. Fishman AJ. Imaging and anatomy for cochlear implants. Otolaryngol Clin North Am 2012;45:1-24. doi: 10.1016/j.otc.2011.08.014.
7. Sennaroglu L, Bajin MD. Classification and current management of inner ear malformations. Balkan Med J 2017;34:397-411.
8. Marsot-Dupuch K, Dominguez-Brito A, Ghasli K, Chouard CH. CT and MR findings of Michel anomaly: Inner ear aplasia. AJNR Am J Neuroradiol 1999;20:281-84.
9. Joshi VM, Navlekar SK, Kishore GR, Reddy KJ, Kumar EC. CT and MR imaging of the inner ear and brain in children with congenital sensorineural hearing loss. Radiographics 2012;32:683-98.
10. Ozgen B, Oguz KK, Atas A, Sennaroglu L. Complete labyrinthine aplasia: Clinical and radiologic findings with review of the literature. Am J Neuroradiol 2009;30:774-80. doi: 10.3174/ajnr.A1426.
11. Hongjian L, Guangke W, Song M, Xiaoli D, Daoxing Z. The prediction of CSF gusher in cochlear implants with inner ear abnormality. Acta Otolaryngol 2012;132:1271-4. doi: 10.3109/00016489.2012.701328.
12. Hwang M, Marovich R, Shin SS, Chi D, Branstetter BF. Optimizing CT for the evaluation of vestibular aqueduct enlargement: Inter-rater reproducibility and predictive value of reformatted CT measurements. J Otol 2015;10:13-17. doi: 10.1016/j.joto.2015.07.004.
13. Ma X, Yang Y, Xia M, Li D, Xu A. Computed tomography findings in large vestibular aqueduct syndrome. Acta Otolaryngol 2009;129:700-8. doi: 10.1080/00016480802412813.
14. Ozgen B, Cunnane ME, Caruso PA, Curtin HD. Comparison of 45 degrees oblique reformats with axial reformats in CT evaluation of the vestibular aqueduct. Am J Neuroradiol 2008;29:30-4.
15. Kesser BW, Raghavan P, Mukherjee S, Carfrae M, Essig G, Hashisaki GT. Duplication of the internal auditory canal: Radiographic imaging case of the month. Otol Neurotol 2010;31:1352-3. doi: 10.1097/MAO.0b013e3181e9bbd2.
16. Takanashi Y, Kawase T, Tatewaki Y, Suzuki J, Yahata I, Nomura Y, Oda K, Miyazaki H, Katori Y. Duplicated internal auditory canal with inner ear malformation: Case report and literature review. Auris Nasus Larynx 2018;45:351-7. doi: 10.1016/j.anl.2017.03.019.